Boundary extraction of linear features using dual paths through gradient profiles

Ryan Lagerstrom *, Changming Sun, Pascal Vallotton

CSIRO Mathematical and Information Sciences, Locked Bag 17, North Ryde, NSW 1670, Australia

ARTICLE INFO

ABSTRACT

An algorithm for automated extraction of linear feature boundaries in 2D images is presented. From a marker set approximating the medial axis, we generate 1D gradient profiles orthogonal to linear features. The algorithm uses dual shortest paths through an image generated from gradient profiles to extract boundaries. The algorithm offers an alternative to a watershed type approach and performs well on images with noise and areas of low contrast. We present the results of our algorithm on microscopy images of neurite outgrowth and other images containing linear features.

Crown Copyright © 2008 Published by Elsevier B.V. All rights reserved.

1. Introduction

The detection of linear features in images is an important activity in the fields of image analysis, pattern recognition and computer vision. Applications are widespread in many realms from remote sensing, microscopy and asset monitoring to biomedical applications. Our particular interest is the detection of linear features in fluorescence microscopy images such as neurite outgrowth in neurons. In this application it is becoming increasingly important to not only count and measure the length of features, but also to extract an accurate boundary for width measurement and for generating masks for co-localisation measurements. The thickness and tapering of neurites is linked with the neuron's electrophysiological response. Measuring neurite thickness is therefore important to support modelling efforts in this area.

There are many existing techniques for linear feature detection in the literature. Thresholding and skeletonisation is a simple method employed, for example by Kim and Gillies (1998) on neural cells. Ridge detection techniques (Eberly, 1996) are used extensively in this area. Guo and Richardson (1998), for example, use ridge detection to find vessels in angiogram images. Exploiting the differential geometry of images, which are treated as surfaces, forms another set of techniques such as those used by Monga et al. (1997) to find linear features in satellite and medical images. Meijering et al. (2004) use differential geometry as the basis of a method for neurite outgrowth analysis. Filtering using mathematical morphology is another effective approach. Soille and Talbot (2001) use directional morphological filtering to detect linear features.

Approaches to linear feature detection often do not produce feature boundaries but instead produce markers or skeletal representations of linear features. The work described in this paper focuses on using these markers to extract the boundaries of linear features. Eiho and Qain (1997), after finding markers for a coronary tree semi-automatically using mathematical morphology, extract feature boundaries using a watershed transformation (Soille, 2003, Section 9.2). Results using a watershed approach can suffer from flooding problems where noise, poor contrast or gaps in linear features exist. Flooding occurs when boundary information is weak and the extracted boundary leaks into the background, see Fig. 3(b). Sonka et al. (1995), using manually identified markers, extract coronary boundaries using a graph searching technique. The graph is constructed from an edge enhanced image produced by a combination of Sobel and Marr-Hildreth operators. The graph searches simultaneously for left and right borders.

This paper proposes an algorithm for automatically extracting the boundaries of linear features in 2D images. Firstly, suitable markers for each linear feature are detected by either an automated process or by manual tracing. The markers are skeletonised and used to estimate local orientation of the features. We then analyse the 1D gradient profiles normal to the local feature orientation. Our algorithm stacks the gradient profiles of a feature into a newly constructed image and uses dual path extraction, as proposed in (Sun and Appleton, 2005), to find the feature boundaries.

Due to constraints we can impose on the dual paths, for example maximum feature width, and the smoothness inherent in shortest paths, our feature boundaries are robust to noise

---

* Corresponding author. Fax: +61 2 9325 3200.
  E-mail address: ryan.lagerstrom@csiro.au (R. Lagerstrom).

degradation or flat areas of an image. A watershed type approach would suffer flooding problems in the presence of these issues.

We present results of our boundary extraction algorithm on microscope images of neurite outgrowth from cells and on a range of images containing linear features from various applications.

2. Boundary extraction using dual paths through 1D gradient profiles

In this section we detail our algorithms for boundary extraction of linear features from marker sets using dual paths through 1D gradient profiles.

2.1. Marker sets

Before extracting boundaries, we require markers for each linear feature. The markers need to be thin, skeleton-like and span the length of each feature of interest. Any of the techniques for linear feature detection described in Section 1 may be used to generate the marker set. Alternatively, manual tracing of each feature center line can be used.

For automated linear feature detection, we use the multiple directional non-maximum suppression (MDNMS) technique proposed in (Sun and Vallotton, 2006). The result of MDNMS forms the basis of our markers for the linear features. The markers are skeletonised (Soille, 2003, Section 5.4) allowing us to separate distinct linear features by removing pixels which have more than two neighbours i.e. branching points. Each distinct linear feature is given a label, and is stored in an image where the pixel value is the label of the feature. The skeletonisation also facilitates local orientation estimation. Fig. 1(b) shows a marker set automatically generated using this method. The results of manually tracing features can similarly be skeletonised to form marker sets.

2.2. Local orientation and 1D profiling

Our algorithm for boundary extraction relies on the generation of 1D profiles normal to the orientation of the linear feature. To do this, we traverse along pixels in the marker set for each linear feature. At each pixel, we look at the two pixels with the same feature label that are a user supplied distance, D, before and after the pixel of interest. The orientation is then estimated as the angle between the horizontal and the line segment joining these two pixels. In the event that a pixel is less than D pixels from the end of a feature, we estimate orientation using the terminating pixel in the feature. The orientation estimates are sensitive to the choice of the value D,
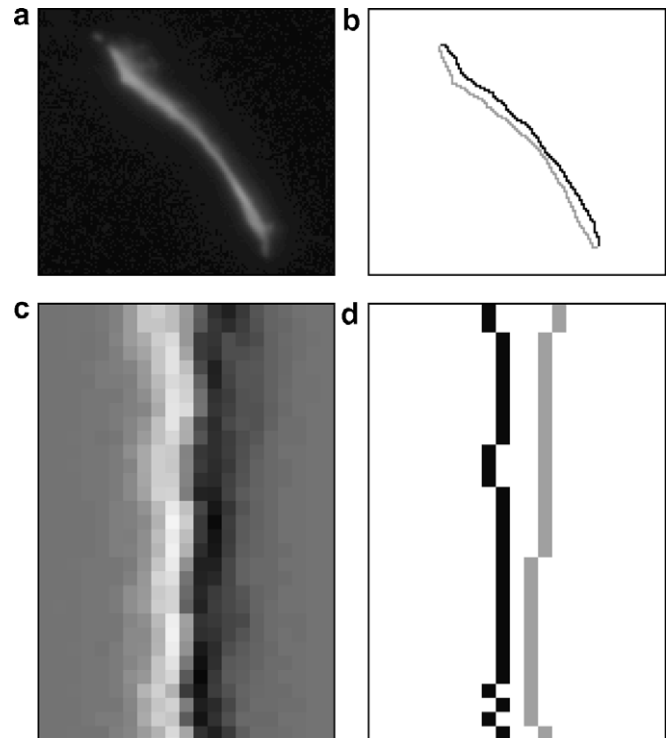
Fig. 2. (a) A single linear feature. (b) Its boundaries extracted using dual paths. (c) A subsection of the stack of 1D gradient profiles. (d) The dual paths found through the subsection.

however the overall algorithm only requires that the estimated orientation leads to a profile that traverses the boundaries of a linear feature. Values of D less than 3 tend to give noisy orientation estimates. We typically set D equal to R, which is discussed in the next paragraph. More robust approaches to estimating local orientation, such as using digital straight lines, may be appropriate but come at a computational cost.

At each pixel, a line with orientation normal to the feature is generated based on the pixel's local orientation estimate. We use Bresenham lines (Bresenham, 1965) to generate the discrete lines which extend a user supplied distance, R, on each side of the feature. The lines sample the pixel values in the original image. The algorithm is sensitive to the choice of R. This parameter needs to be set to a value greater than the radius of the thickest linear feature in the image. We then compute a gradient along each line
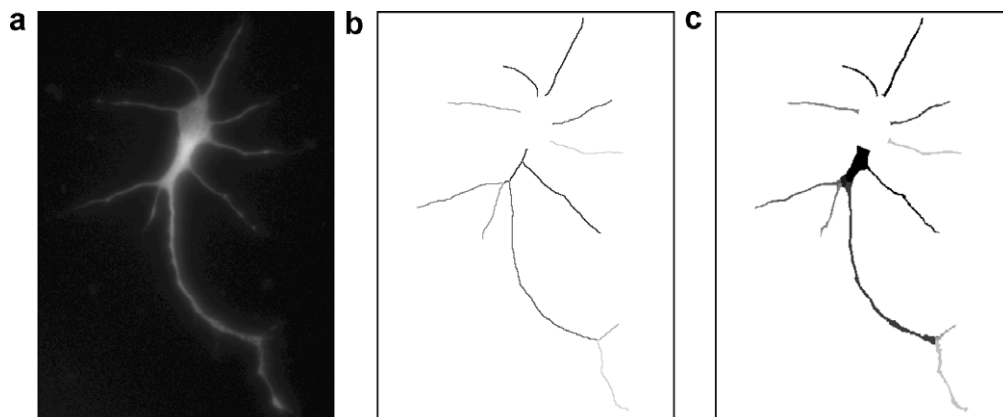
Fig. 1. (a) Neuron image, stained for tubulin (Courtesy of J. Gunnersen, Howard Florey Institute). (b) Marker set, generated using multiple directional non-maximum suppression. (c) Boundaries extracted via the dual paths approach.

using the first derivative weighted by a function of the distance to the center of the feature:

$$G_j = W_j(I_{j+1} - I_{j-1}) \qquad (1)$$

where I_j is the pixel value in the original image along the Bresenham line at offset index j. The offset index has values $j = -R, \ldots, R$. The weight at a particular offset is

$$W_j = (R - |j|)/R \qquad (2)$$

The weighting penalises high gradient values with large distances from their marker. This is useful in that it favours boundaries which are close to their marker in situations where there are multiple features within distance R from each other.

2.3. Dual paths through orthogonal gradient profiles

To extract the boundary of a linear feature, the 1D gradient profiles described in Section 2.2, at each pixel along the marker, are stacked into an image for each feature. Each row of this image corresponds to a gradient profile orthogonal to the marker set. In an ideal case, we would see two distinct lines from the top of the image to the bottom. One of these lines would have high values corresponding to large positive gradients. The other line would have high negative values corresponding to large negative gradients. Fig. 2(c) shows a stack of gradient profiles for the linear feature in Fig. 2(a).

Finding these two distinct lines is a shortest path problem. Sun and Appleton (2005) propose a method for concurrently detecting multiple shortest paths in images. This approach allows us to constrain the regularity of the detected paths for disjointedness, minimal spacing and maximal spacing. Sun and Appleton's method uses an expanded trellis as a search space for multiple paths. The expanded trellis is constrained by a number of geometric and heuristic properties that significantly reduce the complexity and computational burden of the problem.

The cost function for a dual path is the sum of the cost functions of the two single paths as given below:

$$C = \sum_{i=1}^{m} G_{j_i} + \sum_{i=1}^{m} (-1)G_{k_i} \qquad (3)$$

where j_i and k_i are the column position of two paths j and k at row i. G_{j_i} is the value in the gradient profile image at row position i and column position j. The number of rows in the image is represented by m and corresponds to the number of gradient profiles. The following constraints ensure path continuity:

$$|j_i - j_{i+1}| \leqslant A,$$
$$|k_i - k_{i+1}| \leqslant A,$$

while the following constraint ensures the paths are distinct:

$$k_i - j_i > 1.$$

The value of A used in the path continuity constraint is 1. In situations where feature boundaries are irregular or not smooth, this constraint can be relaxed by increasing A to 2 or even 3. However, such an increase comes with a computational cost. The multiplication by negative one of the gradient values, G_{k_i}, in the second term of Eq. (3), guarantees that paths j_i and k_i correspond to positive and negative gradients respectively. Fig. 2(d) shows the dual paths extracted from the gradient profile stack in Fig. 2(c).

Once both paths are detected in the gradient profile image and the extracted paths are mapped back into the original image, path connectivity may be lost. We restore it using a morphological closing with a disc of diameter 3 as a structuring element. The size of the disc was chosen empirically using images of neurites. Neurites do not possess high curvature and it may be necessary to increase this parameter in situations where high curvature is expected. Alternatively, the end points can be joined Bresenham line segments. Fig. 2(b) shows the extracted paths from Fig. 2(d) mapped into the original image.

Fig. 1(c) shows the result of using this approach to find the boundaries of the features in Fig. 1(a) based on the marker set shown in Fig. 1(b).

3. Experimental results

In this section we present results obtained on images of neurite outgrowth and on a range of images containing linear features from various domains.

3.1. Application to neurite outgrowth

The performance of the algorithm was assessed on images of neurite outgrowth. Typically, automated software for quantifying neurite structure does not include width estimates or full segmentation of neurite structure. Instead, only skeletal representations of neurites are supplied. Generating width estimates for neurites
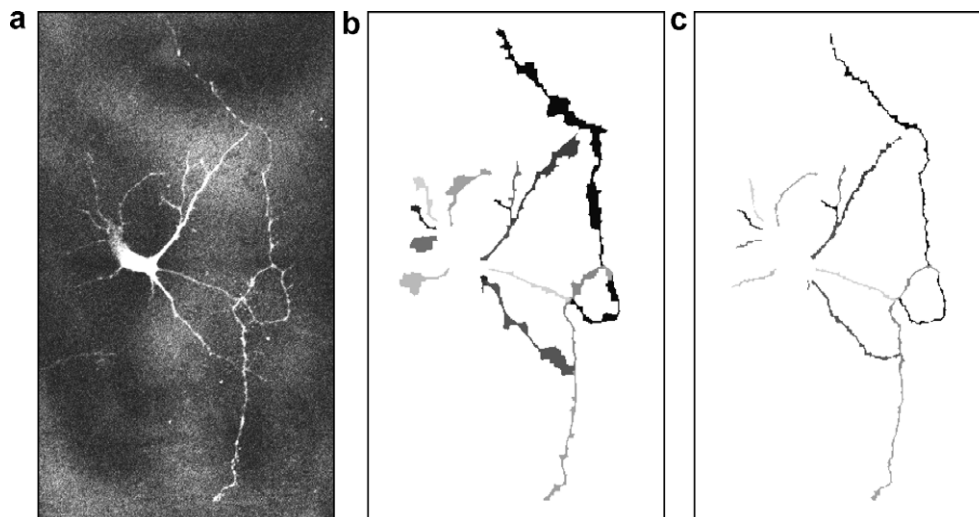
Fig. 3. (a) Neuron image, stained for tubulin (Courtesy of J. Gunnersen, Howard Florey Institute). (b) Boundaries extracted via a watershed approach. (c) Boundaries extracted via the dual paths approach.
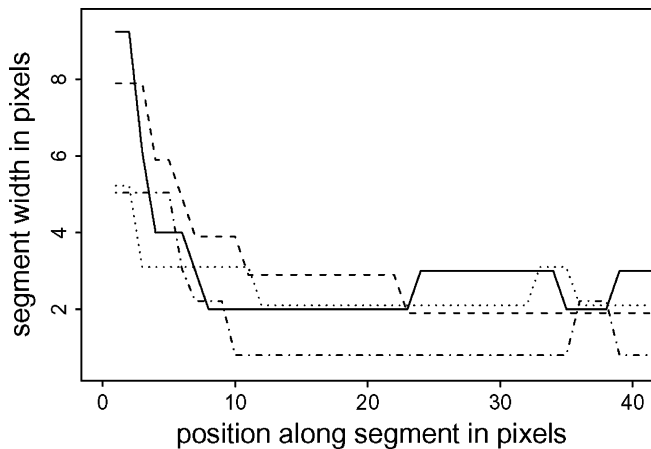
Fig. 4. Plot of taper width along four different neurite segments from Fig. 3(c). Width values are slightly offset for clarity.

allows neuroscientists to automatically discriminate between axons and dendrites, and to profile taper width along neurite structures as they extend away from their parent cell. The extraction of neurite boundaries, along with the subsequent generation of neurite masks, facilitates co-localisation measurements of proteins along the neurite structure.

Two sets of images were used in this study. The first image set consisted of embryonic cortical neurons in culture from Sez-6 null mice. We used the MDNMS approach to generate marker sets for these images. In this example, a line segment length of 15 at 8 angles was used for MDNMS method. An example image from this set is shown in Fig. 1(a) with the result of our approach shown in Fig. 1(c). The parameters R and D were both set to 7. The approach performs well on these images.

The second image set consisted of neurons transfected with an Enhanced Yellow Fluorescence Protein expressing vector. Transfected neurons are plated out together with untransfected neurons so the imaged neurons are effectively sitting on another layer of cells. This makes them harder to trace so we manually generated a marker set for these images. An example image from this set is shown in Fig. 3(a). Fig. 3(b) shows the result of applying a watershed algorithm to extract boundaries. The watershed is performed on a Sobel gradient of the image using the marker set as the foreground seeds. The background seeds are formed from the complement of a dilation of the marker set with radius R, the width parameter used in our method. The approach yields poor boundaries due to the flooding problems caused by noise and saturation. Fig. 3(c) shows the boundaries extracted using the dual paths method.

The parameters R and D were both set to 7. Compared to the watershed approach, there is a vast improvement. The detected boundaries follow the actual object boundaries closely in most instances.

For an image of dimensions 512 by 512 pixels, on an Intel Pentium 4 with 2.66 GHz CPU, the watershed approach takes around 0.1 s. The dual paths method takes around 2 s for the above examples. This method is dependent on the density of features and can take over 10 s for some dense images.

One of the main objectives of this work was to estimate the width of linear features. The width of a feature at any point is estimated by the Euclidean distance between the two boundary pixels along gradient profiles in the original image. To estimate the average width of a linear feature, the average of the widths measured at each pixel along it's marker in the marker set is calculated. The evolution of taper width of a neurite as it extends away from its parent cell is shown in Fig. 4 for a selection of neurites from Fig. 1. For each of four neurite segments, the width at each pixel is plotted and connected by a polygonal line. Also of interest is the ability to count objects within linear structures. Boundary extraction facilitates this measurement as we can produce a mask for linear features. In Fig. 5(a), synapses (stained by synaptophysin) occur along the neurites (stained by tubulin). After applying our method to find the boundaries, Fig. 5(b), we can in turn count the number of black dots (detected synapses) in Fig. 5(c) associated with each linear feature (detected neurites), shown in grey in Fig. 5(c). This provides a measure of synapse density.

3.2. Application to other images

We have also applied our algorithm to images from a range of fields where boundary extraction is required. Figs. 6(a) and (b) show images of a leaf and the extracted boundaries of the leaf veins. The parameters R and D were both set to 12. We used MDNMS to create the marker set in this case with line segment length of 25 at 8 angles. The results allow us to separate the three vein classes based on width measurements. Figs. 6(c) and (d) shows cracks in soil and the results of our boundary extraction approach. The parameters R and D were both set to 12. The marker set was generated using the MDNMS aproach with line segment length of 25 at 8 angles. From the results we can determine a measure for cracking severity based on width. Figs. 6(e) and (f) are aerial images of roads and the boundaries extracted when using our approach. The parameters R and D were both set to 7. The approach yields reasonable results for determining the boundaries of the bright and thick roads but tend to overestimate the width of the thin and dull roads, for example, the road segment in the top center portion of Fig. 6(e).
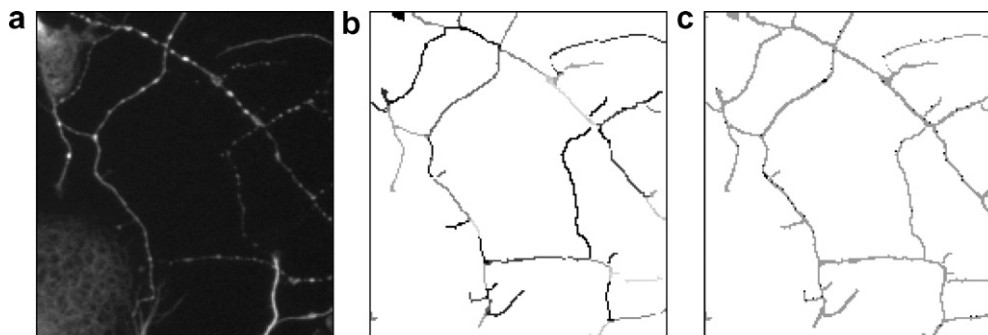
Fig. 5. (a) An image of synaptophysin, appearing as bright dots, alonng neurons (Courtesy of M. Fennel, Wyeth). (b) The result of our boundary extraction method. (c) A mask of the neurons, shown in grey, and synapses which are shown in black.
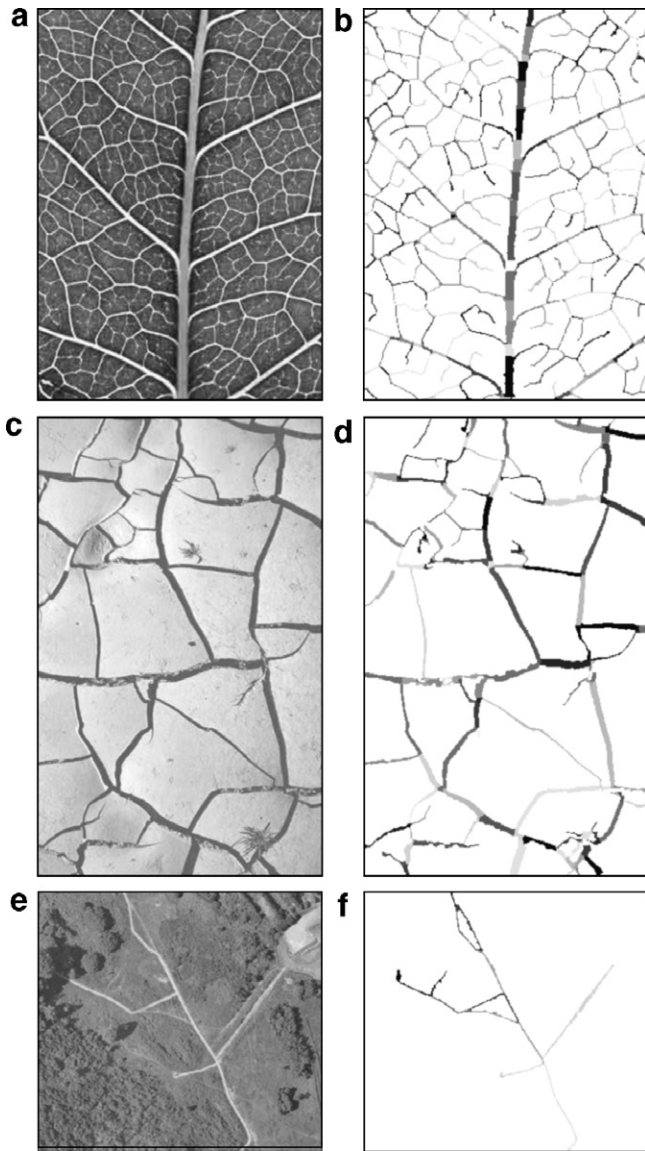
Fig. 6. (a) An image of leaf veins. (b) Extracted vein boundaries. (c) An image of soil cracks. (d) Extracted crack boundaries. (e) An image of roads. (f) Extracted road boundaries.

4. Concluding remarks

We have presented an approach to boundary extraction of linear features. From a marker set, we generate 1D gradient profiles orthogonal to each pixel in the marker. Our approach stacks the profiles into an image and finds dual shortest paths to extract boundaries. The approach compares favourably to standard watershed techniques. We assessed the new technique on images of neurite outgrowth to produce masks of neurites and measure tapering. We also showed the possibilities of the method on a range of images containing linear features.

Acknowledgements

References

Bresenham, J., 1965. Algorithm for computer control of a digital plotter. IBM Systems J. 4 (1), 25–30.
Eberly, D., 1996. Ridges in Image and Data Analysis. Kluwer, Norwell.
Eiho, S., Qain, Y., 1997. Detection of coronary artery tree using morphological operator. IEEE Comput. Cardiol. 24, 525–528.
Guo, D., Richardson, P., 1998. Automatic vessel extraction from angiogram images. IEEE Comput. Cardiol. 25, 441–444.
Kim, J., Gillies, D., 1998. Automatic morphometric analysis of neural cells. Machine Graph. Vision 7, 693–709.
Meijering, E., Jacon, M., Sarria, J.-C.F., Steiner, P., Hirling, H., Unser, M., 2004. Design and validation of a tool for neurite tracing and analysis in fluorescence microscopy images. Cytometry 58A (2), 167–176.
Monga, O., Armande, N., Montesinos, P., 1997. Thin nets and crest lines: Application to satellite data and medical images. Computer Vision Image Understanding 67 (3), 285–295.
Soille, P., 2003. Morphological Image Analysis. Springer, New York.
Soille, P., Talbot, H., 2001. Directional morphological filtering. IEEE Trans. Pattern Anal. Machine Intell. 23 (11), 1313–1329.
Sonka, M., Winniford, M., Collins, S., 1995. Robust simultaneous detection of coronary borders in complex images. IEEE Trans. Med. Imag. 14 (1), 151–161.
Sun, C., Appleton, B., 2005. Multiple paths extraction in images using a constrained expanded trellis. IEEE Trans. Pattern Anal. Machine Intell. 27 (12), 1923–1933. December.
Sun, C., Vallotton, P. Fast linear feature detection using multiple directional non-maximum suppression. In: Proc. Internat. Conf. on Pattern Recognition, vol. 2, IEEE, Hong Kong, 20–24 August 2006, pp. 288–291.